Colloid Polym Sci (2002) 280: 865–872
DOI 10.1007/s00396-002-0695-y

ORIGINAL CONTRIBUTION

Rong-Kun Xia
Wei-Dong He
Cai-Yuan Pan

Amphiphilic particles prepared by grafting acrylamide onto the surface of styrene-rich copolymer/2-hydroxyethyl acrylate rich copolymer particles

Received: 23 May 2001
Accepted: 13 March 2002

R.-K. Xia · W.-D. He · C.-Y. Pan (✉)
Department of Polymer Science and Engineering, University of Science and Technology of China, Hefei, Anhui 230026, China
E-mail: pcy@ustc.edu.cn

Abstract Styrene-rich copolymer/2-hydroxyethyl acrylate rich copolymer [P(St-*co*-HEA)] particles were prepared by emulsifier-free emulsion copolymerization of St with HEA. Fourier transform IR spectroscopy was used to follow the change of HEA content in the particles. The results of X-ray photoelectron spectroscopy measurements indicate that the HEA unit on the surface is richer than that inside the particles. Grafting of acrylamide (AAm) onto the surface of P(St-*co*-HEA) particles was carried out in an aqueous medium containing ceric ions. IR spectroscopy and laser light scattering were used to investigate the grafting polymerization. The morphologies of P(St-*co*-HEA) and P(St-*co*-HEA)AAm particles were observed using a transmission electron microscope. The amphiphilic properties of the particles were characterized by diesel oil and water.

Keywords Amphiphilic particles · Ceric ion · Graft copolymerization · Acrylamide

Introduction

Polymer brushes have attracted much attention because of their unique properties [1, 2] and potential applications in new adhesive materials [3, 4], protein-resistant biosurfaces [5], chromatographic devices [6], lubricants [7], polymer surfactants [8] and polymer compatibilizers [8]. Brush polymers have two essential components: the anchoring surface and the anchored chains. This work concentrated on spherical brushes. Qualitatively, a spherical polymer brush has the same morphology as a core–shell polymer [9, 10]. Generally, covalent attachment can be accomplished by either "grafting-to" or "grafting-from" approaches. In the former approach, the end functional group of the polymer molecules reacts with an appropriate substrate to form polymer brushes. In general, only a small amount of polymer can be immobilized onto the surface by this approach because the polymer chains must diffuse through the existing polymer film to reach the reactive sites on the surface, as the tethered polymer film thickness increases, the barrier becomes important. As a result, a low grafting density of the brush polymer is obtained. Compared with the grafting-to approach, the grafting-from approach is a promising method and is accomplished by the immobilized initiator which initiates the polymerization of the monomer. Among the technologies used in the grafting-from approach, the best one is free-radical graft copolymerization [11, 12, 13, 14]. For example, Ballauff and coworkers prepared spherical polyacrylic acid (PAA) brushes by photoemulsion polymerization. First, a polystyrene (PSt) latex was prepared by conventional emulsion polymerization. In the second step, seeded emulsion polymerization was performed using 2-[*p*-(2-hydroxy-2-methylpropiophenone)]-ethylene glycol methacrylate, which acts as a photoinitiator. The third step was photoemulsion polymerization in the presence of AA. This graft-from process produced a PSt core with a shell of linear PAA brushes [15]. In order to achieve better control of the molecular weight and the molecular-weight distribution of the polymer brushes, controlled radical polymerizations including atom-transfer radical polymerization (ATRP), reverse ATRP, nitroxide-mediated stable free-radical polymerization and iniferter radical polymerizations have been used to synthesize tethered polymer brushes on solid surfaces [16, 17, 18, 19]. Although the grafting-from approach using conventional and controlled radical polymerization can prepare polymer brushes, the immobilization of the initiator on the surface involves several steps, which may lead to a low graft density of initiators and tethered polymers if the reaction is not quantitative. Also side reactions, which may occur in the initiator immobilization reaction, will introduce some undesired structures on the surface. The lack of knowledge about the exact composition of the initiator layer makes the understanding of the polymerization mechanism difficult in some cases. This work reports a method where the copolymer with initiator on the surface of particles was prepared by emulsifier-free emulsion polymerization and the grafting copolymerization of acrylamide (AAm) was performed in the presence of ceric ammonium nitrate. As we know, the initiation system containing alcohol and Ce(IV) shows high reactivity in aqueous media and has been applied in the preparation of block and graft copolymers. Recently, this method was used for the surface grafting of AAm onto glycol-carrying particles to produce hairy particles [20]. The polymerization mechanism involves complex formation between Ce(IV) and a reducing agent, followed by the generation of a free radical which initiates the polymerization of vinyl monomer [21]. The reducing agent may be starch [22], cellulose [23], chitin [24], poly(vinyl alcohol) [25], poly(ethylene glycol) [26], ketonic resins [27], etc. It is well known that PAAm is a water-soluble polymer. Grafting AAm onto various polymer backbones such as guar gum, starch, carboxymethyl cellulose and xanthan gum, etc. can modify their properties [28, 29]. In our research group, a series of copolymer microspheres with hydrophilic polymer on the surface was prepared by emulsifier-free emulsion copolymerization of styrene (St) with methacrylic acid, acrylonitrile, hydroxylethyl (meth)acylates [HE(M)A], etc, [30, 31, 32, 33, 34]. In this work, P(St-*co*-HEA) microspheres of submicrometer size were prepared by emulsifier-free emulsion copolymerization. Then grafting of AAm onto the surface of P(St-*co*-HEA) microspheres was carried out successfully. The morphologies and the properties of spherical brushes were investigated.

Experimental

Materials

St (Shanghai Chemical Co, C.R) and HEA (Aldrich, C.R.) were purified by distillation under reduced pressure. AAm (Shanghai Chemical Co, C.R.) was recrystallized from distilled water. Ammonium persulfate (APS), ceric ammonium nitrate, $Ce(NH_4)_2(NO_3)_6$ (CAN), and other organic chemicals were all of analytical grade and were used without further purification. The diesel oil was $0^{\#}$. A calculated amount of CAN was dissolved in 1N HNO_3 aqueous solution to prepare 0.1 M stock solution and this was stored in a refrigerator.

Preparation of P(St-*co*-HEA) microspheres

P(St-*co*-HEA) microspheres were prepared by emulsifier-free emulsion copolymerization of St with HEA using APS as an initiator. The recipes of the copolymerization are listed in Table 1. The reaction was carried out under a nitrogen atmosphere at 70 °C for 7 h with mechanical stirring at 350 rpm. The copolymer microspheres were purified by repeating dialysis for at least 1 week.

Preparation of polymer microspheres grafted with AAm[P(St-*co*-HEA)AAm]

A typical procedure of grafting polymerization is as follows [34]. AAm (5 g) dissolved in 40 ml distilled water was mixed with 10 ml latex containing 0.5 g P(St-*co*-HEA) (HEA2 in Table 1) with constant stirring, and the mixture was flushed with a slow stream of N_2 for about 15 min. An aqueous solution of CAN (5 ml, 0.1 mol/l) was added into the reaction system while stirring. The reaction was carried out at 30 °C under a nitrogen atmosphere in the dark for a prescribed time and was then terminated by adding a saturated solution of hydroquinone. Several drops of the reaction mixture were withdrawn and diluted with water. After ultrasonic dispersion, transmission electron microscope (TEM) observation and laser light scattering (LLS) measurement were conducted. The graft copolymerization conditions and results are listed in Table 2. At the end of the reaction, the graft polymer microspheres were precipitated by adding latex into excess acetone, then filtered, and

Table 1. Recipes and results of preparing styrene-rich copolymer/2-hydroxyethyl acrylate rich copolymer [*P(St-co-HEA)*] microspheres at 70 °C for 7 h

Sample	Styrene (g)	2-Hydroxyethyl acrylate (g)	Ammonium persulfate (g)	H_2O (ml)	Conversion (%)[a]	C_{COO}/C_{total} (%)	
						Theoretical[b]	X-ray photoelectron spectroscopy
HEA1	10	1.6	0.048	100	92.5	1.65	1.89
HEA2	10	3	0.048	100	96.4	2.88	3.13

[a] The total conversion of styrene and 2-hydroxyethyl acrylate was measured by gravimetry

[b] Assuming that styrene and 2-hydroxyethyl acrylate are copolymerized homogenously, the theoretical ratio is $C_{COO}/C_{total} = \left[\left(\frac{W_{HEA}}{M_{HEA}}\right)/\left(\frac{W_{St}}{M_{St}}\times 8+\frac{W_{HEA}}{M_{HEA}}\times 5\right)\right]\times 100\%$, where W_{St} and W_{HEA} are the weights of monomers styrene and 2-hydroxyethyl acrylate added and M_{HEA} and M_{St} are the molecular weights of 2- hydroxyethyl acrylate and styrene, respectively

Table 2. Grafting polymerization of acrylamide (*AAm*) onto P(St-*co*-HEA) particles. Polymerization conditions: HEA2: 0.5g; AAm: 3 g; ceric ammonium nitrate (0.1 mol/l): 5 ml; 30 °C

Sample	t (h)	Conversion (%)[a]	Laser light scattering		Size increase of graft polymer	
			R_h[b]	dw/dn[c]	Diameter increase (nm)	ΔV (%)[d]
HEA2	–	–	125.4	0.0502	–	–
AAM1	6	14.5	130.3	0.0702	9.8	12.2
AAM2	12	29.2	134.1	0.0218	17.4	22.3
AAM3	18	32.1	134.8	0.0141	18.8	24.2
AAM4	24	35.6	135.3	0.0030	19.8	25.6

[a] Conversion (%) = $(W_{graft}-W_{HEA2})/W_{HEA2}\times100\%$, where W_{graft} and W_{HEA2} are the weights of grafting polymer and HEA2 particles

[b] R_h is the hydrodynamic radius

[c] dw/dn is used to characterize the size distribution of the polymer particles

[d] $\Delta V(\%) = (V_{graft}-V_{HEA2})/V_{HEA2}\times100\%$

put in acetone overnight while stirring in order to remove unreacted AAm. The grafting copolymer particles were collected by filtration, washed with a mixture of formamide and acetic acid (1:1 v/v) to remove the homoPAAm [29], and dried in a vacuum oven at 70 °C for about 24 h. In comparison, the polymerization of AAm was performed with the same conditions of grafting polymerization except the polymer latex was not added. No polymer was isolated after polymerization at 30 °C for 24 h.

Characterization

The size measurement and morphology observation of P(St-*co*-HEA) microspheres and graft copolymer microspheres [P(St-*co*-HEA)AAm] were performed using a Hitachi-800 TEM. A modified commercial LLS spectrometer (ALV/SP-125) equipped with an ALV-5000 multi-t digital time corrector and a solid-state laser (DPSS, output power about 400 mV at 532 nm) was used to measure the size of the polymer microsperes. In dynamic LLS, the cumulant analysis of the measured intensity–intensity time correlation function, $G^{(2)}(t,q)$, in the self-beating mode results in a linewidth distribution $G(\Gamma)$. For a pure diffusive relaxation, $(\Gamma/q^2)_{q\to0,c\to0}$ leads to the translational diffusion coefficient, D, or further to the hydrodynamic radius, R_h, via the Stokes–Einstein equation. The details of LLS theory can be found elsewhere [35, 36]. IR spectra were recorded using a VECTOR-22 spectrometer. The X-ray photoelectron spectroscopy (XPS) analysis was carried out with an ESCALAB MarKΠ system with a residual pressure of 3×10^{-9} mbar. The analyzer was in the constant resolution mode at a pass energy of 20 eV. The slit width of the analyzer was 6 mm. A Mg Kα radiation source ($h\nu = 1{,}253.6$ eV) was used with an overall energy resolution of 1.2 eV. The samples used in this measurement were dried in a vacuum oven at 50 °C for 24 h and then stored in a vacuum desiccator. The amphiphilic properties of the microspheres were characterized by soaking the dry polymer microspheres in diesel oil or water and then measuring the weight increase by gravimetry.

The weight increase ratio = [(soaked polymer weight-dry polymer weight)/dry polymer weight] × 100%.

Results and discussion

Preparation of P(St-*co*-HEA) microspheres

P(St-*co*-HEA) microspheres were prepared by emulsifier-free emulsion copolymerization of St and HEA. Their IR spectra (HEA1 and HEA2 in Table 1) shown in Fig. 1 reveal well-defined characteristic bands of the St unit. A characteristic peak at 1,731 cm^{-1} is attributed to carbonyl stretching of carboxylic groups, verifying the copolymerization of HEA and St. With the increase in the HEA content in the copolymerization system (HEA1→HEA2), the intensity ratio of the peak at 1,731 cm^{-1} to that at 1,452 or 1,493 cm^{-1}, which is ascribed to the skeletal vibrations of benzene ring in the St unit, clearly increases, suggesting that much HEA was copolymerized with St. As a result, the microspheres have a higher content of HEA.

In order to graft AAm onto the surface of P(St-*co*-HEA) particles, it is necessary to estimate the distribution of the hydroxyl groups on the surface. XPS was used to investigate the surface functionality, and the results for HEA2 are shown in Fig. 2. The full-scan spectrum in Fig. 2a indicates that the main elements on the particle surface are carbon and oxygen (hydrogen

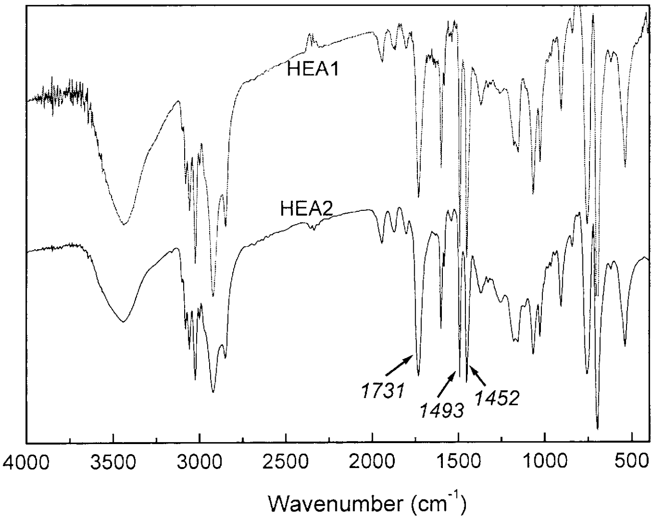

Fig. 1. IR spectra of styrene-rich copolymer/2-hydroxyethyl acrylate rich copolymer [*P(St-co-HEA)*] microspheres HEA1 and HEA2 in Table 1

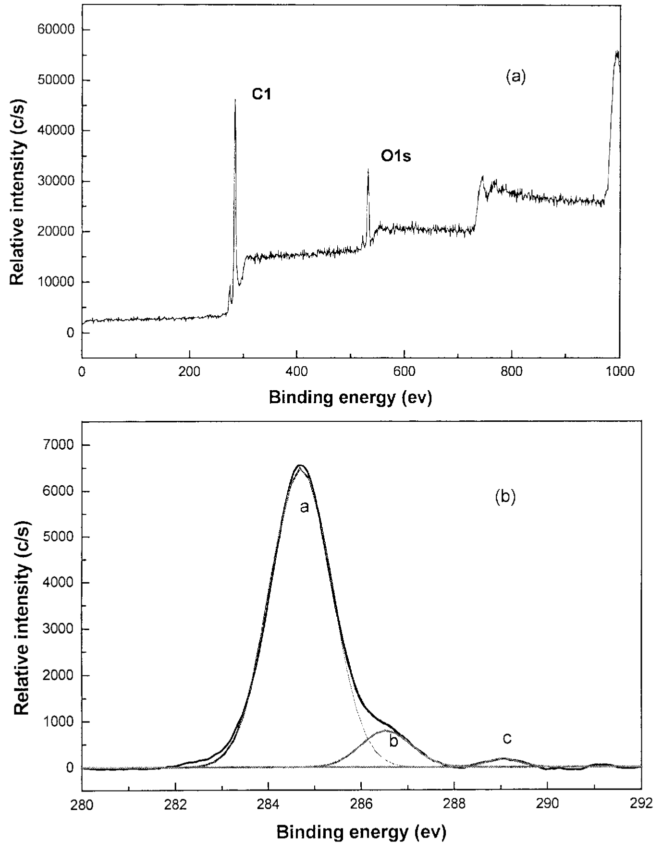

Fig. 2. **a** The full-scan X-ray photoelectron spectroscopy spectrum and **b** the C1*s* spectrum of P(St-*co*-HEA)

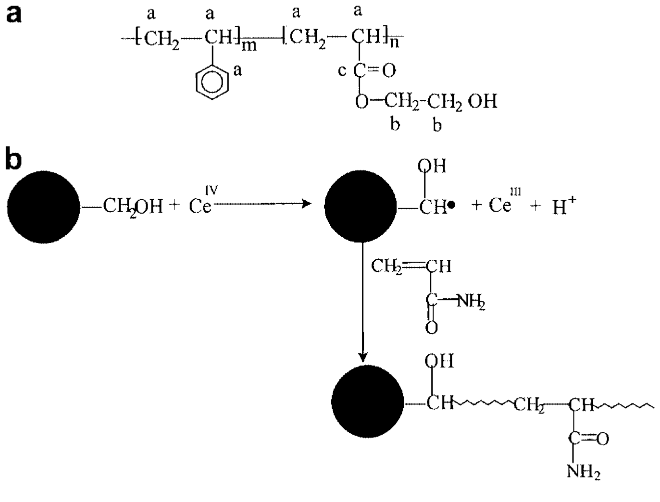

Scheme 1. The graft copolymerization route

cannot be detected by XPS). Shape analysis of the C1*s* spectrum in Fig. 2b reveals three peaks, with binding energies at 284.7, 286.58 and 289.05 eV, corresponding to three types of carbons in this copolymer as shown in Scheme 1a [31, 37, 38]. The peak at 289.05 eV in Fig. 2b corresponds to carbon of the carboxylate group. As we know, the HEA unit in the copolymer contains one carboxylate group and one hydroxyl group. Thus, we can calculate the hydroxyl group concentration on the surface on the basis of the carbon data of the carboxylate group. The ratio of the number of carboxylate carbons in HEA unit to all the carbons of the St and HEA units in the copolymer, C_{COO}/C_{total}, could be calculated from the percentage of carbon at 289.05 eV against all the carbon atoms at 284.7, 284.58 and 289.05 eV in Fig. 2b. The results listed in Table 1 show that with an increase in the feed ratio of HEA/St (HEA1→HEA2), the ratio of C_{COO}/C_{total} on the surface increases (1.89→3.13%). The higher values for the surfaces of HEA1 and HEA2 than the corresponding theoretical values (Table 1) demonstrate more HEA on the surface compared with in the core of the particles. Kamei and coworkers [39, 40] reported that the emulsifier-free emulsion copolymerization of St and HEMA proceeded via two-stage polymerization. In the early stage of polymerization, HEMA-rich copolymer was formed in an aqueous medium and precipitated to form particles. Then, the St-rich copolymer produced was precipitated onto the particles, and nonspherical particles with the surface covered by HEMA-rich and St-rich copolymers were obtained. When considering this mechanism of particle formation, it is easier to understand that the ratio of C_{COO}/C_{total} on the surface layer of the particles was much lower than 0.2. This value was calculated based on the assumption that the surface of the particles was completely covered by HEA. A similar result was obtained by other researchers [33, 41].

Preparation of polymer microspheres grafted with AAm[P(St-*co*-HEA)AAm]

The grafting copolymerization of HEA2 with AAm was carried out in an aqueous solution containing ceric ions. In comparison, polymerization of AAm with the same conditions and feed ratios of graft copolymerization was performed except P(St-*co*-HEA) latex was not used, and no polymer was formed. A similar result was also obtained by Desmukh et al. [28]. So the grafting polymerization must be the result of a free radical in the surface HEA unit produced by disproportionation of coordination complexes between ceric ions and alcohol initiating the polymerization of AAm [43] (Scheme 1), and homopolymer formation in solution would be negligible. For studying the grafting polymerization process, the samples were withdrawn from the polymerization system at prescribed time intervals and measured by IR spectroscopy, TEM and LLS. The IR spectra of HEA2 in Table 1 and AAM1–AAM4 in

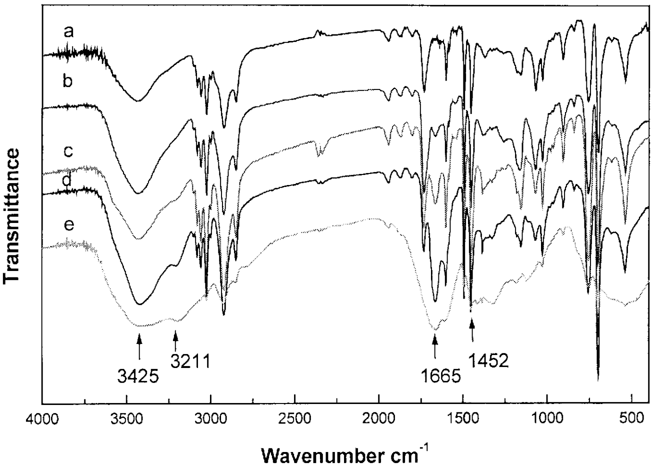

Fig. 3. IR spectra of HEA2 (*a*) in Table 1, AAM1 (*b*), AAM2 (*c*), AAM3 (*d*) and AAM4 (*e*) in Table 2

Table 2 are shown in Fig. 3. In Fig. 3, spectra b–e, we found three additional bands, the two bands at 3,429 and 3,211 cm^{-1} represent the $-NH_2$ group (one for symmetrical and the other for antisymmetrical stretching of N–H bonds) and the band at 1,665 cm^{-1} is ascribed to the carbonyl group of the AAm unit, other than the characteristic bands of St and HEA units, indicating the formation of the graft copolymer. During the grafting copolymerization, the amount of St did not change, so the band at 1,452 cm^{-1} was used as a reference. Plotting the peak height ratio of $H_{1,665}/H_{1,452}$ against the polymerization time affords Fig. 4. The value of $H_{1,665}/H_{1,452}$, i.e., the relative content of AAm in the P(St-*co*-HEA)AAm particles increased continuously as the grafting copolymerization progressed. In the conventional free-radical polymerization, this should be the result of more initial sites on the surface of the particles participating in the initiation. The probable reason is that as more AAm molecules are grafted, the surface of the P(St-*co*-HEA)AAm particles becomes very hydrophilic, which favors the contact of ceric ions with the alcohol group.

The growth of the P(St-*co*-HEA)AAm particles was followed by LLS. R_h and d*w*/d*n* were calculated and are listed in Table 2. The relation of R_h and the distribution of the particle size with reaction time is shown in Fig. 5. The percentage of the average volume increase of each particle, ΔV, and the variation of d*w*/d*n* with polymerization time shown in Fig. 6 demonstrate that the increase in the particle volume was faster for 12-h polymerization after addition of the initiator and then leveled off as grafting polymerization proceeded. This phenomenon is different from the IR data in Fig. 4, which shows a bigger increase in PAAm even after 12-h polymerization. Probably this is reasonable. As we know, the increase in the diameter of the particles is determined by the chain length of hairy PAAm. In the initial period of grafting polymerization, the hairy PAAm is sparse, and will lie down on the surface. With the progress of grafting polymerization, the grafting density increases and hairy PAAm chain will stand up and gradually stretch because the hairy PAAm becomes crowded. Thus, the increment of the particle size is bigger. When more AAm molecules are grafted onto the surface with the crowded hairy PAAm chains, the increment of the particle size is only due to stretching of the hairy chains, resulting in a smaller size increment. In order to explain the uniform trend of the particle size in the course of the polymerization as shown in Fig. 5, the particle morphologies of samples HEA2 and AAm1–AAm4 were

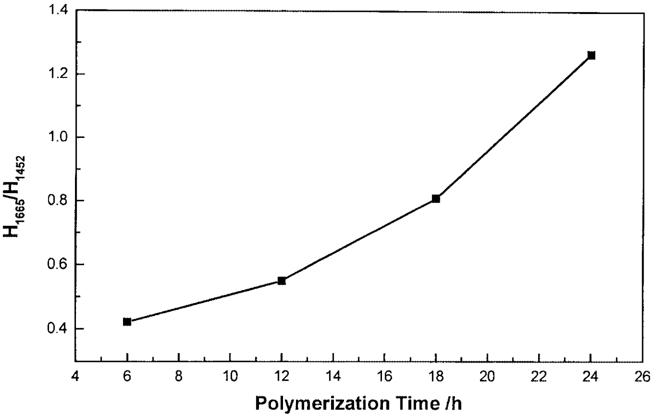

Fig. 4. The relationship between H_{1665}/H_{1452} and polymerization time. The conditions are listed in Table 2

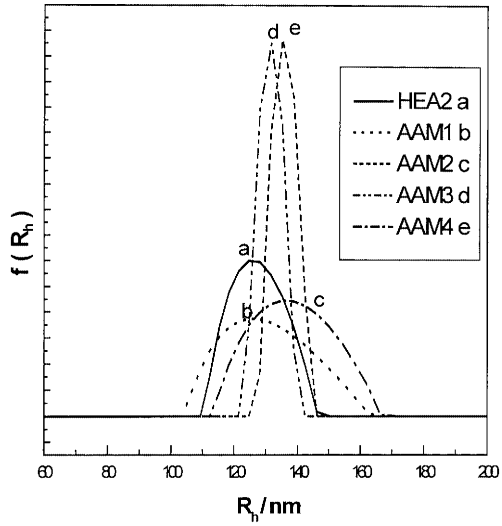

Fig. 5. The effect of grafting polymerization time on R_h and the size distribution of P(St-*co*-HEA)AAm particles. Polymerization conditions: see Table 2

Fig. 6. The variation of $(V_{\mathrm{graft}}-V_{\mathrm{HEA2}})/V_{\mathrm{HEA2}}$ and dw/dn with polymerization time. Polymerization conditions: see Table 2

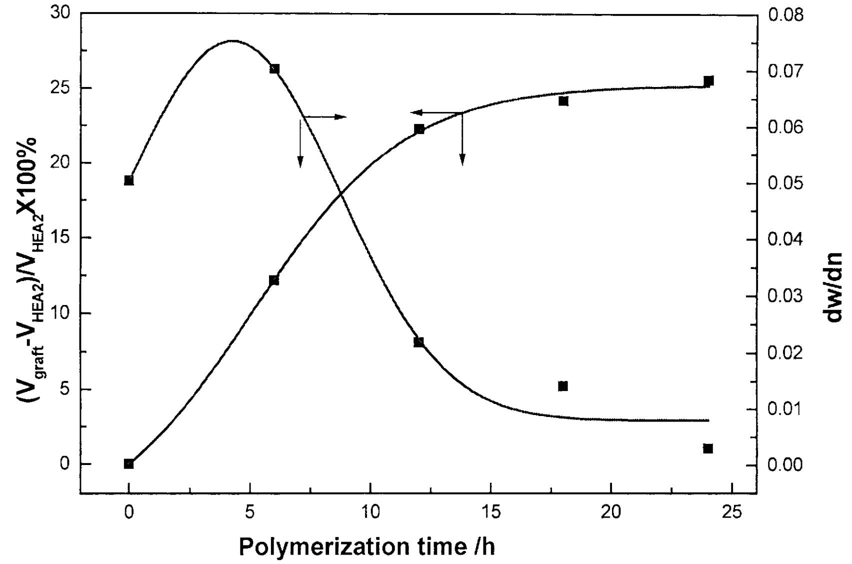

observed using a TEM, and their photographs are shown in Fig. 7. We can find from Fig. 7a that some small particles are attached to bigger particles. In the initial period of grafting polymerization (before 6 h polymerization), the grafted PAAm changes the surface properties, and some small particles were detached from the bigger particles (Fig. 7b), and all the particles grew. The grafting of PAAm onto the surface and the detaching of particles from bigger particles occur at the same time, resulting in the distribution of the particle size becoming broader than that of the original HEA2 (Fig. 5, curves a and b). After 12-h polymerization, the detaching action had almost finished; this can be observed in Fig. 5, curve d. The continuously grafting polymerization of AAm results in the formation of uniform particles (Fig. 5, curves b–e), probably owing to the disappearance of almost all the large particles attached to the small particles. In addition, the small particles have more possibilities to initiate the polymerization of AAm because of their larger surface area at the same weight. It should be interesting to study the surface properties of the particles. When hydrophobic core P(St-*co*-HEA) is covered by hydrophilic polymer PAAm, the diesel oil absorbability of the particles should decrease with the increase of the hydrophilic polymer covered on the surface[44]. If the particle surface is completely covered by PAAm, and the hydrophilic polymer layer is thick enough, the particles will not absorb organic liquid. The changes in the absorbabilities in water and diesel oil of the amphiphilic particles with grafting polymerization time are shown in Fig. 8. As the polymerization time increases, the water absorbability increases and the diesel oil absorbability decreases. The increase in the water absorbability and the decrease in the diesel oil absorbability reflect the increase in the hydrophilic PAAm grafting onto the surface of the hydrophobic core. Obviously, a big decrease in the diesel oil absorbability from 6 to 12-h polymerization demonstrates the quick increase in the area covered by PAAm.

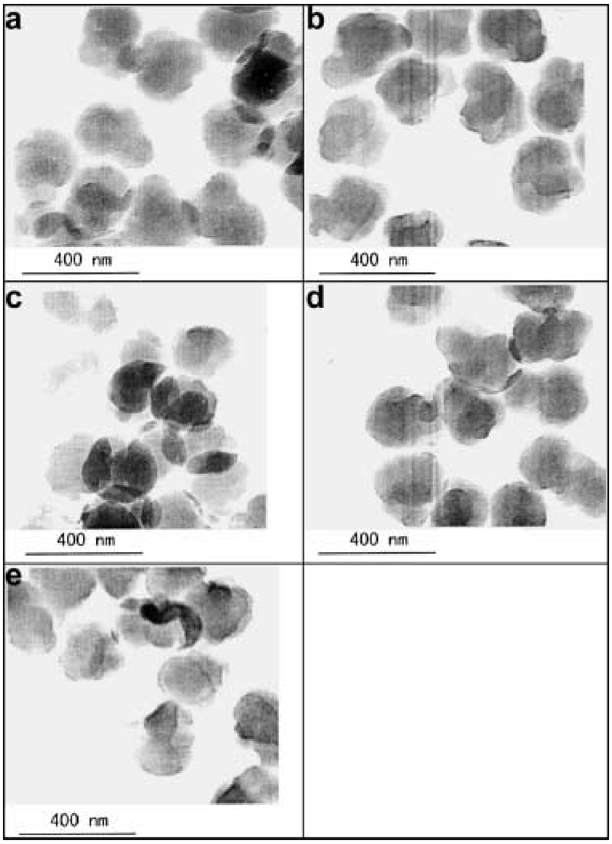

Fig. 7. Transmission electron microscopy photographs of **a** HEA2 in Table 1, **b** AAM1, **c** AAM2, **d** AAM3 and **e** AAM4 in Table 2

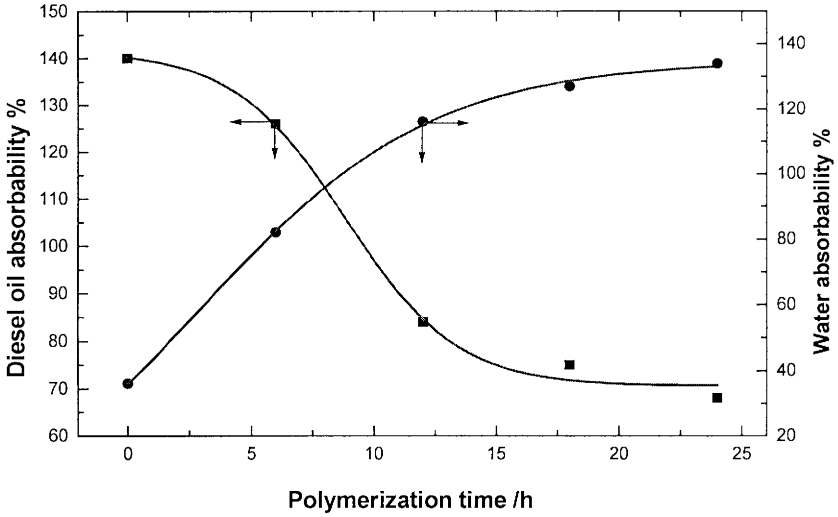

Fig. 8. Effect of polymerization time of grafting AAm onto the surface of particles on the water and diesel oil absorbabilities of the P(St-*co*-HEA)AAm articles

Conclusions

Irregular P(St-*co*-HEA) particles with the surface rich in HEA were prepared by emulsifier-free emulsion copolymerization of St and HEA. As the feed ratio of HEA/St increases, the amount of PHEA on the surface increases. Free radicals on the surface of the P(St-*co*-HEA) particles produced by disproportionation of coordination complexes between ceric ions and alcohol of the HEA unit could initiate the polymerization of AAm in water, and P(St-*co*-HEA) grafted with AAm was obtained. With the increase of grafting polymerization time, the amount of PAAm grafted and the thickness of the PAAm layer on the surface of the particle increase. This must be the result of more initiation sites on the HEA units participating in the initiation of AAm. As more PAAm chains are grafted onto the surface of the particles, the water absorbability increases, and the amount of diesel oil absorbed by the hydrophobic core decreases, but the product obtained after 24-h grafting polymerization still has diesel oil absorbability although the absorbability decreases greatly.

Acknowledgement This research work was supported by the National Natural Science Foundation of China with grant 50173025.

References

1. Halperin A, Tirrell M, Lodge TP(1992) Adv Polym Sci 100:31
2. Takei YG, Aoki T, Sanui K, Ogata N, Sakurai Y, Okano T (1994) Macromolecules 27:6163
3. Raphaël E, de Gennes PG (1992) J Phys Chem 96:4002
4. Gi H, de Gennes PG (1993) Macromolecules 26:520
5. Amigi M, Park KJ (1993) Biomater Sci Polym Ed 4:217
6. Van Zanten JH (1994) Macromolecules 27:6796
7. Goanny J-F (1992) Langmuir, 8:989
8. Milner ST (1991) Science 251:905
9. Johnson J, Hassander H, Tornell B (1994) Macromolecules 27:1932
10. Marion P, Beinert G. Juhue D, Lang J (1997) Macromolecules 30:123
11. Prucker O, Ruhe J (1998) Macromolecules 31:602
12. Prucker O, Ruhe J (1998) Macromolecules 31:592
13. Jayachandran KN, P.R.Chatterji (2000) Eur Polym J 36:743
14. Zhang J, Uchida E, Uyama Y, Ikeda Y (1995) Langmuir 11:1688
15. Guo X, Weiss A, Ballauff M (1999) Macromolecules 32:6043
16. Nakayama Y, Matsuda T (1996) Macromolecules 29:8622
17. Ejaz M, Yamamoto S, Ohno K, Tsujii Y, Fukud T (1998) Macromolecules 31:5934
18. de Boer B, Simon HK, Weits MPL, Van der Vegte EW, Hadziioannou I (2000) Macromolecules 33:349
19. Sedjo RA, Mirous BK, Brittain WJ (2000) Macromolecules 33:1492
20. Matsuoka H, Fujimoto K, Kawaguchi H (1999) Polym J 31:1139
21. Story RF, Goff LT (1989) Macromolecules 22:1058
22. Vera-Pacheco M, Vasquez-Torres I, Cauche-Escamilla G (1993) J Appl Polym Sci 47:53
23. Arthur JC (1985) Encylopedia of polymer science and technology, vol 3, 2nd edn. Wiley, New York, p 68
24. Lagos A, Yazdani-Pedram M, Reyes J (1992) J Macromol Sci Pure Appl Chem A 29:1007
25. Chowdhury P, Pal CM (1999) Eur Polym J 35:2207
26. Srinivasan KSV, Nagarajan S (1995) J Polym Chem 33:2925
27. Akar A, Galioğlu A, Göçmen A, Saraç AS (1990) J Appl Polym Sci 39:1657
28. Deshmukh SR, Sudhakar K, Singh RP (1991) J Appl Polym Sci 43:1091
29. Tripathy T, Pandey SR, Karmakar NC, Bhagat RP, Singh RP (1999) Eur Polym J 35:2057
30. Wang PH, Pan CY (2000) J Appl Polym Sci 75:1693
31. Wang PH, Pan CY (2000) Colloid Polym Sci 278:245
32. Wang PH, Pan CY (2000) Colloid Polym Sci 278:581

33. Wang YM, Pan CY (2001) Eur Polym J 37:699
34. Wang PH, Pan CY (2001) Colloid Polym Sci 279:98
35. Chu B (1991) Laser light scattering, 2nd edn. Academic, New York
36. Berne B, Pecora R (1991) Dynamic light scattering, 2nd edn. Plenum, New York
37. Li L, Chan C-M, Weng LT (1997) Macromolecules 30:3698
38. Beamson G, Briggs D (1992) High-resolution XPS of organic polymers. The Scienta ESCA300 database. Wiley, New York
39. Kamei S, Okubo M, Matsumoto T (1986) J Polym Sci Polym Chem Ed 24:3109
40. Okubo M, Yamamoto Y, Uno M, Kamei S, Matsumoto T (1987) Colloid Polym Sci 265:1061
41. Ceska GW (1974) J Appl Polym Sci 18:427
42. Santos AMD, Mckenna TF, Guillot J (1997) J Appl Polym Sci 65:2343
43. Arslan H, Hager B (1999) Eur Polym J 35:1451
44. Li H-Q, Zhao G, Ruckenstein E (1999) Colloids Surf 161:489